A Millimeter Wave Backscatter Network for Two-Way Communication and Localization

Haofan Lu
UCLA
haofan@cs.ucla.edu

Mohammad Hossein Mazaheri
UCLA
mhmazaheri@cs.ucla.edu

Reza Rezvani
UCLA
reza.r@ucla.edu

Omid Abari
UCLA
omid@cs.ucla.edu

ABSTRACT

Millimeter wave (mmWave) technology enables wireless devices to communicate using very high-frequency signals. Operating at those frequencies provides larger bandwidth which can be used to enable high-data-rate links, and very accurate localization of devices. However, radios operating at high-frequencies consume significant amount of power, making them unsuitable for applications with limited energy sources. This paper presents MilBack, a backscatter network operating at mmWave bands. Backscattering is the most energy-efficient wireless communication technique, where nodes piggyback their data on an access point's signal instead of generating their own signals. Eliminating the need for signal generation significantly reduces the energy-consumption of the nodes. In contrast to past mmWave backscatter work which supports only uplink, MilBack is the first mmWave backscatter network which supports uplink, downlink, and accurate localization. MilBack addresses the key challenges that prevent existing backscatter networks to enable both uplink and downlink at mmWave bands. We implemented MilBack and evaluated its performance empirically. Our results show that MilBack is capable of achieving accurate localization, uplink, and downlink communication at up to 8 m while consuming only 32 mW and 18 mW, respectively.

CCS CONCEPTS

• **Hardware** → **Wireless devices**; **Beamforming**; *Digital signal processing*; • **Networks** → *Wireless access points, base stations and infrastructure*;

KEYWORDS

mmWave Backscatter Communication, Integrated Sensing and Communication, Localization, Orientation Sensing, Two-way communication

1 INTRODUCTION

Millimeter wave (mmWave) technology refers to very high frequency (typically 24 GHz to 100 GHz) signals. Over the past decade, there has been much interest in using this technology in wireless networks. mmWave networks have three advantages over traditional wireless networks. First, they provide much higher network throughput since they can benefit from a large bandwidth available in the high-frequency spectrum. In fact, Federal Communications Commission (FCC) has released more than 14 GHz of bandwidth for both licensed and unlicensed use in the mmWave frequency bands above 24 GHz, which is orders of magnitude more than the bandwidth allocated to today's WiFi networks [1]. Second, mmWave networks can provide connectivity to many nodes simultaneously on the same frequency band. In particular, due to the small wavelength of mmWave signal (millimeter scale), mmWave antennas are tiny and hence it is possible to pack hundreds of antennas in a small area, creating an antenna array with a very directional beam. Using directional beams for communication enables mmWave networks to perform space division multiplexing to support multiple links simultaneously, on the same frequency band [20, 39, 43, 50]. Third, thanks to the short wavelength of mmWave signals, and the availability of large bandwidth and narrow beams, mmWave networks can perform very accurate localization (both range and direction) of their devices, which has the potential to open up many new opportunities and applications.

Despite the above advantages, existing mmWave networks have a major limitation that makes them unsuitable for many IoT applications. mmWave radios have high power consumption, and hence they cannot be used in devices with limited energy sources. The problem is intrinsic, as the power consumption of Radio Frequency (RF) circuits is proportional to their operating frequencies [26], and therefore most components of a radio, such as mixers and oscillators, consume much more power when they run at such high frequencies. Additionally, in contrast to traditional radios, mmWave radios require steerable directional antennas (such as phased arrays), which significantly increase the power consumption of these radios [23, 54].

To overcome the high power consumption problem of mmWave networks, researchers have designed mmWave backscatter devices [35, 45]. The vision is to design mmWave devices that can piggyback

their data on a mmWave signal emitted by an access point (AP), instead of generating and transmitting their own signals. Eliminating the need for an active transmitter and power-hungry RF components has enabled mmWave backscatter devices to communicate on a very low energy budget. However, exiting mmWave backscatter devices enable either accurate localization or only uplink communication [12, 35, 41, 45]. Hence, they cannot be used in applications which need both uplink and downlink connectivity such as Virtual Reality (VR) and Augmented Reality (AR). To the best of our knowledge, no current mmWave backscatter system enables localization, uplink, and downlink communications altogether.

In this paper, we introduce MilBack, the first mmWave backscatter network which enables localization, uplink, and downlink communication. MilBack's design consists of a novel backscatter node and an access point (AP). MilBack supports both uplink and downlink communication between its AP and nodes. It also enables accurate localization and orientation sensing of nodes. MilBack achieves this by introducing multiple key innovations:

1) Two-Way Backscatter Communication and Localization: The first challenge is to develop a low-power backscatter node which can enable two-way communication and localization. To achieve this, MilBack introduces a novel backscatter node architecture, including a passive mmWave structure which creates two directional beams while the beams can operate in absorptive or reflective mode. In the absorptive mode, the node receives the AP's signal using its two beams and passes it to its novel and simple baseband processor for demodulation. This enables downlink communication from the AP to the node. In the reflective mode, each beam reflects only a specific frequency component of the AP's signal back to the AP, where these frequencies depend on the orientation of the node with respect to the AP. This enables the AP to estimate the location and orientation of the node by transmitting a wide-band signal and monitoring which frequencies are reflected back to it. Finally, by switching the beams' mode between reflective and absorptive, the node modulates the AP's signal and reflects it back to the AP, supporting uplink communication.

2) Orientation Assisted Quadrature Frequency Modulation (OAQFM): The second challenge is to develop a modulation scheme which enables the backscatter node to modulate or demodulate signals using a very simple and low-power baseband processor. To achieve this, MilBack introduces a new modulation scheme called Orientation Assisted Quadrature Frequency Modulation (OAQFM). Typical modulation schemes (such as QAM) use cosine and sine (with the same frequency) to present complex symbols, and hence they require a mixer and oscillator to separate the cosine and sine components and modulate/demodulate the signal. Unfortunately, due to the complexity and power consumption of these components, these modulation schemes are not suitable for mmWave backscatter nodes. In contrast, MilBack introduces OAQFM, a modulation scheme, which instead of using cosine and sine, uses two cosines (tones) but at different frequencies to represent complex symbols. This enables the MilBack's node to receive these tones from the AP using its beams, and then modulate or demodulate it using simple low-power envelope detectors (power detectors) integrated at the output of its passive directional reflector/absorber.

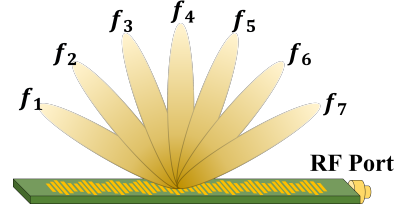In this paper, we make the following contributions:

Figure 1: Frequency Scanning Antenna (FSA). FSA passive structure creates beams where their directions depends on the frequency of the signal. Here, we show beams for only seven frequencies, however, FSA enables continuous beam directions across its frequency band.

- We introduce the first mmWave backscatter system which enables localization, orientation sensing, uplink, and downlink communication.
- We present a new modulation scheme for mmWave backscatter node which exploits the orientation of the nodes, and two single-tone signals to enable two-way communication between the AP and nodes.
- We design a two-port mmWave structure which operates in reflective or absorptive mode. We integrate it with off-the-shelf components to build MilBack's node and the AP. We evaluate MilBack performance in real-world scenarios.

Our empirical evaluation shows that MilBack achieves accurate localization, downlink, and uplink communication while consuming only 18 mW and 32 mW, respectively, which is significantly lower than power consumption of past mmWave backscatter networks which only supports uplink [35].

Ethics Statement: This paper does not raise any ethical concerns or issues.

2 BACKGROUND

In this section, we provide some background on topics related to MilBack.

FSA Technology: Frequency Scanning Antenna (FSA) is a passive structure that creates a beam where its direction depends on the frequency of the signal, as shown in Figure 1. Said differently, as the frequency of the received/transmitted signal changes, the direction of the beam changes too. Moreover, if the signal includes two or multiple different frequencies, the structure creates two or multiple different beams, where the direction of each beam corresponds to that specific frequency. FSA structure consists of an array of emitting elements. As the signal propagates through the structure, it experiences phase shifts between the consecutive emitting elements. Therefore the emitting signals will combine constructively over the air, creating a beam. However, as the frequency of the signal changes, the amount of phase shift between two consecutive emitting elements changes too. Therefore, the direction in which signals combine constructively (i.e. the direction of the beam) will change with the frequency of the signal. FSA has been mostly used in imaging and weather radars to enable multi-dimensional environment sensing and imaging [21, 55]. Recently, it has also been
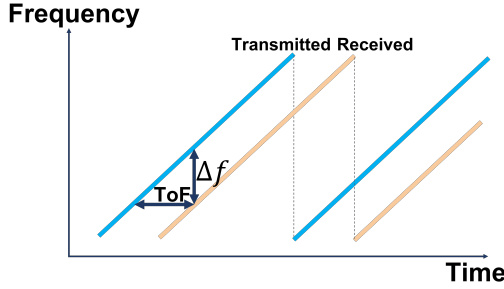
Figure 2: FMCW Radar Signal. FMCW radar transmits a chirp signal (blue). The signal gets reflected back by an object, and the radar receives the delayed version of it (orange). The time-of-flight (ToF) can be discovered from the frequency difference between the transmitted and received signal.

used to enable passive beamforming for relays [28]. Another recent work [37] has also explored using FSA in localization and user identification; however, their design requires 10 GHz bandwidth to cover 48° azimuth angle. MilBack builds on past work on FSA, and design a *dual-port mmWave* FSA to achieve passive and low-power beamforming for backscatter networks. Our FSA design covers over 60° azimuth angle with only 3 GHz bandwidth.

FMCW Technology: Frequency Modulated Continuous Wave (FMCW) radar is one of the most widely adopted wireless sensing technology [8–11, 42]. This radar technology can measure the distance of objects from itself by transmitting a signal and measuring the reflection from the objects. To do so, the FMCW radar transmits a chirp signal whose frequency changes linearly with time as shown in Figure 2. This signal goes over the air and gets reflected back by an object. The radar receives the reflected signal and compares its frequency to that of the transmitted signal. This comparison is done simply by multiplying the transmitted signal with the received signal and checking the frequency of the result. Note, since the transmitted signal frequency is changing linearly in time, delays in the reflected signals translate into frequency shifts in comparison to the transmitted wave as shown in Figure 2. Therefore, by comparing the frequency difference between the transmitted signal and the received signal, one can discover the time delay that the signal incurred which corresponds to the time-of-flight (ToF) from the radar device to the object. In particular, ToF can be calculated as follow: $ToF = \Delta f / slope$, where Δf is the measured frequency difference between the transmitted and received signal, and slope is the slope of the frequency sweep as shown in Figure 2. Finally, once the ToF is computed, the radar can estimate the round-trip distance of the object from itself by multiplying the ToF with the speed of light. Note, although the above description is for a single object, it can be extended to an environment with multiple objects.

3 MILBACK OVERVIEW

In contrast to past mmWave backscatter systems which enable either localization or communication (only uplink), we introduce MilBack, the first mmWave backscatter network which enables uplink, downlink and accurate localization of its backscatter devices. MilBack network includes an AP and one or multiple backscatter

nodes. The node operates in two modes: reflective or absorptive. In the reflective mode, it reflects the AP's signal back to the AP. This enables the AP to accurately estimate the distance, direction and orientation of the nodes. In particular, the AP uses directional antennas to create transmitting and receiving beams. Then, it steers these beams together while transmitting its signal. When the beams are facing toward a node, the node reflects the signal back to the direction of arrival (i.e. direction of the AP). The AP receives the backscattered signal and accurately estimate the distance, direction, and orientation of the node using FMCW. MilBack then exploits the orientation information of the node and enables both uplink and downlink communication between its nodes and AP using its novel low-power design and modulation scheme.

Over the next few sections, we will explain how MilBack works in details. We first present MilBack's backscatter node design, and discuss how it creates a reflective or absorptive beam toward the AP without using active mmWave components such as phased arrays. We then explain how the AP can estimate the location and orientation of the backscatter nodes. Next, we described how MilBack's low-power low-cost node enables both uplink and downlink communication. Finally, we explain MilBack's protocol to enable two-way communication and localization.

4 MILBACK'S NODE DESIGN

Due to the high-frequency nature of mmWave signals, these signals decay quickly with distance. Hence, a backscatter node operating at mmWave frequency needs to focus its reflected power into a narrow beam toward the AP in order to compensate for the path loss. Otherwise, the AP does not hear the node's reflected signal. A typical approach to create and steer beams in mmWave nodes is to use phased arrays. However, phased arrays are complex and power-hungry to be used in a low-power backscatter node. Hence, past work has proposed to use the Van Atta technique to create a beam in backscatter nodes [12, 35, 45]. Van Atta is an array of antennas that are connected to each other through transmission line traces. This passive structure can create a beam and reflect signals in the same direction as their arrival direction [44]. However, we cannot use Van Atta in our design. In particular, Van Atta designs are targeted only for reflecting signals and they cannot be used for receiving since the do not have any signal ports. Therefore, although they are great options for backscatter nodes that enable only localization or uplink, they are not suitable for MilBack which targets both uplink and downlink.[1]

To solve the above problem and create beams passively while supporting both uplink and downlink, our idea is to build a backscatter node using the FSA structure. As described in section 2, FSA is a passive structure which creates a beam where the direction of the beam depends on the frequency of the signal. FSA does this without consuming any power which makes it ideal for low-power designs such as backscatter nodes. Moreover, as shown in Figure 1 FSA has a signal port which can be used to receive and feed the signal to a receiver to enable downlink. In contrast to a typical FSA, described

---

[1]In Van Atta, the length of traces between antennas should be carefully tuned. Thus, we cannot easily insert switches and/or ports in the middle of the traces to direct the signal to a local processor for downlink.
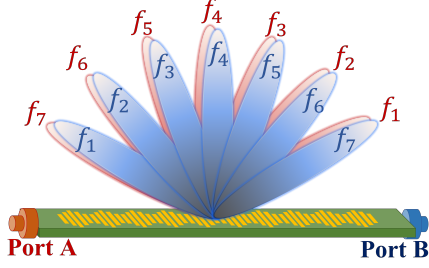
Figure 3: Beam Pattern of the MilBack's Dual-Port FSA. Our dual-port FSA enables creating two sets of beams while their frequency assignments are mirror of each other.
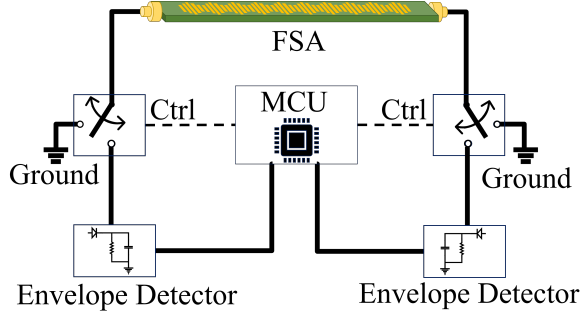

Figure 4: Block Diagram of a MilBack's Backscatter Node. Our design is simple and low-power since it does not require power hungry mmWave components such as amplifiers, mixers and oscillators.

in section 2, we design and build a *dual-port* FSA for MilBack's backscatter nodes.

Dual-port FSA: The FSA structure is symmetric, and hence by adding a second port to the other side of the FSA structure, we can enable two sets of beams as shown in Figure 3. The red beams are created by Port A and the blue beams are created by Port B. Therefore, for each direction, there will be two beams that correspond to different frequencies. For instance, in Figure 3, the rightmost beam corresponds to frequency f_1 and f_7 for Port A and Port B, respectively. As we describe in the following sections, this dual-port FSA will enable MilBack to sense the orientation of nodes as well as support higher data-rate uplink and downlink communication.

The node's architecture: Figure 4 shows the block diagram of a MilBack's backscatter node. Our design consists of a dual-port FSA antenna where each of its ports is connected to a switch. Each switch connects the FSA port to either the ground plane of the FSA (i.e. short circuit) or an envelop detector. When the FSA ports are connected to the ground, the FSA's beam reflects the signal back to the AP. On the other hand, when the FSA ports are connected to the envelope detectors, the FSA's beam absorbs the AP's signal and passes it to the envelop detector. Hence, the node does not reflect any signals. This is because the envelope detector has a 50 ohm input impedance which is matched with the impedance of the FSA's

port. Finally, the outputs of the envelop detectors are connected to the ADC pin of a micro-controller unit (MCU) which also controls the switches. Note, the design is simple, low-cost, and low-power. It does not use any costly and power-hungry mmWave components such as phased arrays, phase shifters, amplifiers, oscillators, or mixers. All it needs is two envelop detectors, two switches, and a low-power processor unit (such as a micro-controller).

5 LOCALIZATION AND ORIENTATION

MilBack is able to find the location and orientation of its nodes with respect to its AP.

5.1 Location Detection

To find the location of a node with respect to the AP, MilBack uses FMCW as described in section 2. In particular, the AP transmits an FMCW chirp signal while the node is in reflective mode. Then the AP measures the reflected signal from the node and estimates the signal's time-of-flight and the distance of the node with respect to itself. However, to do this, MilBack needs to address a challenge; MilBack's AP needs to extract the node's reflected signal from the reflection of other objects in the environment. In particular, the node's reflection is much weaker than the reflection of some other objects.

To solve the above challenge, we use a similar technique as the background subtraction technique used in radar systems [10]. In our design, the node switches between reflective and absorptive mode at 10 KHz rate (i.e. modulating the reflected signal) while the AP is transmitting FMCW chirps. The AP then takes the FFT of the received signal of five consecutive chirps, and subtract every two pair from each other. It then uses the results of these subtractions to detect the node's reflected signal. Note, since the chirp duration is much shorter than any changes in the environment, the subtraction will remove the reflected signals of other objects. On the other hand, since the node's reflection is modulated, it will experience changes between consecutive chirps. Hence, the node's reflected signal will not be removed by subtraction. Using this technique, the AP can detect the node's reflection from the signal reflected by other objects, and estimate the distance of the node with respect to itself.

5.2 Orientation Detection

The orientation sensing of a node can be crucial for applications such as VR and AR in determining user's gesture and direction. MilBack enables both the AP and the node to estimate the orientation of the node with respect to the AP.

(a) AP detecting node's orientation: MilBack's design enables its AP to estimate the orientation of the node. To do so, the AP transmits an FMCW signal while the node operates in the reflective mode. Recall that the node's beam direction depends on the frequency of the signal. Therefore, the node creates a reflective beam toward the AP only for some specific frequencies of the FMCW signal. Said differently, the node reflects only some frequencies of the FMCW signal back to the AP where those frequencies depend on the orientation of the node with respect to the AP. Hence, the AP

can estimate the orientation of the node by monitoring which frequencies of the FMCW signal have resulted in the highest reflection power.

Similar to the localization process, here we also need to distinguish between the node's reflected signal and the reflection by other objects. Therefore, we put one port of the node's FSA in absorptive mode and switch the other port between absorptive and reflective mode to create different reflected signals over time. This enables the AP to take the FFT of the signal and perform background subtraction. After removing the background, the AP then takes an IFFT and measures the reflected signal power across MilBack's mmWave FMCW band. This enables the AP to measure which signal frequency has resulted in the highest reflection power and use it to accurately estimate the orientation of the node.

(b) Node detecting its own orientation: MilBack design enables the node to also estimate its own orientation with respect to the AP. To do so, the node needs to find out which one of its beams is aligned toward the AP. Recall that the node uses FSA to passively create beams where their directions depend on the frequency of the signal. Moreover, for the beams which are aligned toward the AP, the node receives the highest power from the AP. Therefore, there is a one-to-one mapping between the orientation of the node and the signal frequency which results in the highest received power at the node. Now the question is how the node can measure which signal frequency results in the highest received power.

The AP transmits an FMCW signal while the node is measuring the received signal power using its envelope detector. Note, although the envelop detector can measure the received power, it cannot identify the frequency of the signal. Hence the node cannot detect which frequency has resulted in the highest received power. To solve this issue, our idea is to use a triangular chirp instead of the sawtooth chirp for the FMCW signal. In this case, although the node cannot measure the frequency of the signal which resulted in the highest received power, it can measure the delay between the two times when the node receives the highest power, as shown in figure 5. In particular, the V-shape property of the triangular chirp creates different delays between the two peaks in the received power where the amount of the delay depends on the orientation of the node. This enables the node to measure the delay and estimate its orientation. In the following section, we explain how this orientation information is used at the AP to choose correct carrier frequencies for both uplink and downlink communication.

6 COMMUNICATION

Past backscatter mmWave systems enable either localization or communication (only uplink). In the previous section, we explained how MilBack enables localization and orientation sensing. In this section, we explain how MilBack also enables both downlink and uplink communication using its novel architecture.

6.1 Downlink Communication

Due to the significant path loss of mmWave signals, any mmWave transmitters and receivers must focus their energy into narrow beams to compensate for the loss. Therefore, communication is only possible once their transmitter and receiver beams are aligned. Recall that MilBack's node uses our dual-port FSA to passively
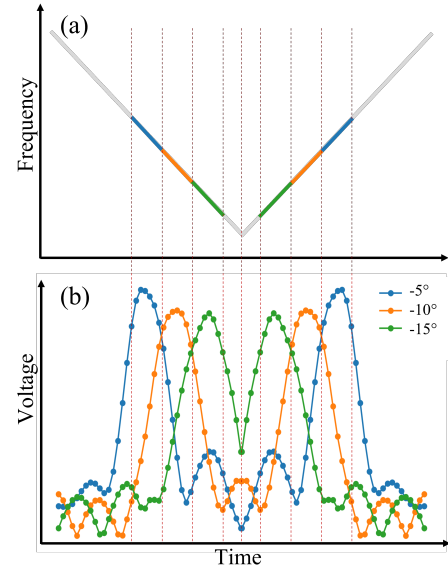

Figure 5: Orientation Detection at the Node. (a) a triangular FMCW waveform, and (b) received signal power at the output of the node's power detector for three different node orientations.

create two beams as shown in Figure 3, where the direction of each beam depends on the signal frequency, and the signal of each beam is received by only one of the port. Hence, for the AP to send data to the backscatter node, the AP first needs to know which two signal frequencies to use for communication. In particular, one frequency aligns the beam for the Port A of the FSA toward the AP while the other frequency aligns the beam for the Port B of the FSA toward the AP. Note, these frequencies can be selected based on the orientation of the node. In particular, the AP estimates the nodes' orientation by measuring the reflected signal power across different frequencies as described in Section 5.2. The frequencies which have resulted in the highest reflected power are the frequencies that have aligned the node beams toward the AP. Once the AP chooses the correct frequencies to align the node's beams toward the AP, it can then send signals at those frequencies which are received at two ports of the node's FSA. As shown in Figure 4, each port is connected to a dedicated envelope detector which enables a simple micro-controller to demodulate and decode the signal in a simple and low-power approach as we describe next.

6.2 OAQFM

MilBack takes advantage of the two-port FSA and introduces a new modulation technique, called Orientation Assisted Quadrature Frequency Modulation (OAQFM). In this technique, the AP encodes its bits by modulating two carrier signals, where their frequencies are selected based on the orientation of the node. In particular, the presence or absence of each carrier signal can be used to present four different symbols, as shown in an example in Figure 6. In this example, the AP has selected f_A and f_B frequencies for communication since they have aligned the node's beams toward the AP. Here, if the AP wants to send bits "01" or "10", it transmits a single tone
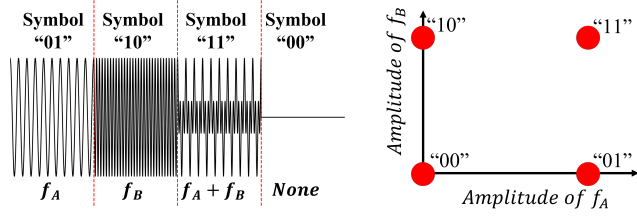
Figure 6: OAQFM Modulation. it uses the presence or absence of two tones (f_A and f_B) to represent different symbols.

at f_B or f_A, respectively. Similarly, if it wants to send bits "11", it transmits two tones at f_A and f_B, simultaneously.

On the node side, each port of the FSA is connected to a switch which can connect the FSA port to either ground or an envelop detector, as shown in Figure 4. In the downlink mode, the switch connects the FSA ports to envelop detectors whose outputs are connected to the micro-controller. This enables the node to measure the power of the signal received by each port. Since each port receives only one of the carrier frequencies (f_A or f_B), the node can seamlessly decode the bits by checking the presence or absence of a signal at each of the two FSA ports.

So far we explained how MilBack enables downlink communication by introducing dual-port FSA and OAQFM modulation. However, in cases where the node is normal to the AP (i.e. zero incidence angle), the FSA's beams for port A and Port B will be operating at exactly the same frequency (i.e. $f_A = f_B$). Hence, the AP cannot use two carrier frequencies in these cases and need to use a single carrier frequency. Note, we already explained how the AP and the node can estimate the orientation of the node. Therefore, when they sense that the node is normal to the AP, they both rely on a single carrier on-off-keying (OOK) modulation.

6.3 Uplink Communication

MilBack enables low-power uplink communication between its nodes and AP using the backscattering technique. In particular, the AP transmits a query signal consisting of two tones at frequencies that align the node's beams toward the AP. Then the node uses the OAQFM modulation to piggyback its data on the AP's query signal by selectively reflecting or absorbing each tone. For example, to send '01' to the AP, the node reflects the tone at f_A while absorbing the tone at f_B. Similarly to sending '10' to the AP, the node reflects the tone at f_B while absorbing the tone at f_A. Finally, to send '00' the node absorbs both tones, and to send '11' it reflects both tones. Now, the question is how the node can change each beam to absorptive or reflective mode, independently?

Recall that each FSA port is connected to a switch which connects the port to either the ground plane or an envelope detector. Moreover, each port receives only one of the tones in the AP's query signal. Hence, when an FSA port is connected to the ground, the FSA reflects back the tone which corresponds to that specific port to the AP. On the other hand, when the FSA port is connected to the envelope detector, the FSA absorbs that tone since the input impedance of the envelop detector is matched with the impedance of the FSA's port. Therefore, the node can switch each beam to
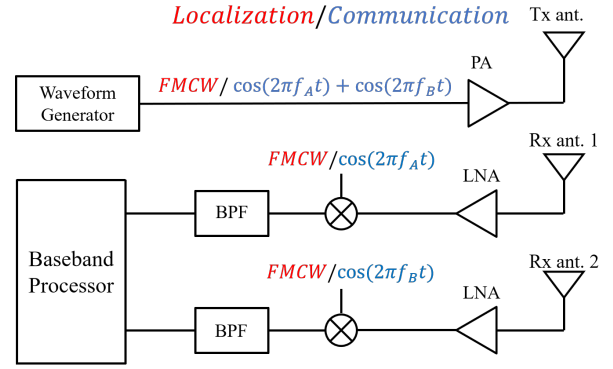

Figure 7: Block Diagram of MilBack's AP.

reflective or absorptive mode independently by connecting each FSA port to either ground or the envelop detector.

So far we have explained how the node can modulate the AP's signal and encode its data using OAQFM. However, when the AP receives the node's signal, it first needs to extract it from interference signals. There are two types of interference in our system. The first one is self-interference which is caused by the AP itself. This is due to the fact that the AP is receiving the node's weak signal while transmitting a strong query signal. The second one is caused by the signals reflected by other objects, such as walls and desks in the environment, which also creates interference to the node's signal. To mitigate this interference at the AP, our idea is to multiply the received signal with each tone of the AP's query and then filter out the interference as we explain in the following.

Figure 7 shows the block diagram of MilBack's AP. The AP transmits a query signal consisting of two tones (i.e. $cos(2\pi f_A t) + cos(2\pi f_B t)$) using one antenna and receives the reflected signals using two antennas. The signal at each receiving antenna is first amplified using an LNA and then multiplied by one of the query signal's tones using a mixer. Note, since the interference signals (both the self-interference and reflection from surrounding objects) are just a delayed version of the transmitted signal, when they are multiplied by the tone (e.g. $cos(2\pi f_A t)$), the results will be a DC signal and some high-frequency signals (i.e. $cos(2\pi 2 f_A t)$, $cos(2\pi f_{A+B} t)$ and $cos(2\pi f_{A-B} t)$) which can be easily filtered out using a band pass filter (BPF). On the other hand, the node's reflected signal is the modulated version of the AP's transmitted signal. Hence, when the AP multiplies it by the tone, the results will be some high-frequency signals (which are filtered out using BPF) and the node's response at baseband frequency. Therefore, by doing this, the AP can easily extract the node's response from interference signals.

7 TWO-WAY COMMUNICATION AND LOCALIZATION PROTOCOL

Previous sections presented different components of MilBack, enabling localization and two-way communication between its backscatter nodes and the AP. Here, we explain MilBack's joint communicating and localization protocol.
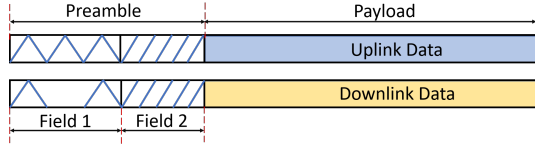
Figure 8: MilBack Packet Structure. Preamble is used for localization, sensing the node's orientation, and informing the node whether the system operates in uplink or downlink mode.

MilBack packets consist of a preamble followed by a payload, as shown in Figure 8. The preamble includes two fields: Field 1 and Field 2. The purpose of the first field is to enable the node to estimate its orientation and also inform the node whether the AP will send or receive data during payload. The purpose of the second field is to enable the AP to localize the node. Finally, the payload will carry the uplink or downlink data.

During the first field of the preamble, the AP sends multiple triangular FMCW chirps while the node has its ports (beams) in the absorptive mode. This enables the node to sense its orientation, and the AP to inform the node whether the system will operate in the uplink or downlink mode during the payload. In particular, if the AP sends three chirps during this field, it means that the system operates in the uplink mode. In this case, during the payload part of the packet, the AP sends a query signal (i.e. two tones) while the node modulates it and sends its data to the AP as described in 6.3. On the other hand, if the AP sends two chirps (with a gap in the middle, as shown in the figure 8) during the first field, it means that the system operates in the downlink mode. In this case, during the payload, the AP sends data and the node receives and decodes it as described in section 6.1. During the second field of the preamble, as shown in Figure 8, the AP sends five FMCW sawtooth chirps while the node switches its ports between the reflective and absorptive mode. This enables the AP to receive the node's reflection and localize it and sense its orientation as described in section 5. Following the preamble, there will be a payload which is used either for uplink or downlink. The length of the payload is predefined for both AP and the nodes, however, it can be adjusted based on the application and data-rate requirements. Finally, it is noteworthy that MilBack can potentially support multiple nodes by using spatial division multiplexing (SDM) technique. In particular, the AP can create multiple beams towards different nodes and establish communication links with them concurrently.

8 IMPLEMENTATION
In this section, we explain the implementation of MilBack's node and AP in details.
MilBack Node: Figure 9 shows the prototype of our MilBack's node. We implemented the node using off-the-shelf circuit components and our customized dual-port FSA antenna. For the FSA design, we reproduced an FSA designed by a past work [28], and extend their design to a dual-port FSA. We evaluated the design using ANSYS HFSS software and fabricated it on a PCB using Rogers Substrate. For the two switches, we used ADRF5020 SPDT RF Switch [5], which enables the node to connect the FSA ports to either short circuit or the envelop detectors. For the envelope detectors, we
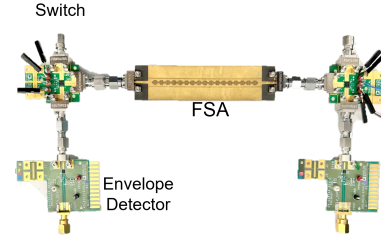

Figure 9: MilBack's Node Implementation. Our prototype uses evaluation boards for switches and envelope detectors. However, one can design a compact prototype of MilBack's node by integrating all components on the same PCB board as the FSA.

used ADL6010 [2] which has 50 Ω input impedance, matched to the FSA impedance. Finally, we used a TI MSP-EXP430FR6989 [3] module as a low-power microcontroller on the node to control the switches and process the downlink and uplink data.

MilBack AP: Figure 7 shows the block diagram of MilBack's AP. For waveform generation, we used a Keysight M9384B VXG which can generate the FMCW signal for localization, and the two-tone signal for communication. The signal is then amplified using an Analog Device ADPA7005 power amplifier [4] and fed to a directional antenna. The signal power is 27dBm. Each FMCW chirp takes 45 μs and 18 μs in Field 1 and Field 2 of the preamble, respectively. We have chosen slower chirps for Field 1 since the sampling rate of the node's microcontroller is lower than the AP's sampling rate. Each chirp spans 3 GHz bandwidth from 26.5 GHz to 29.5 GHz[2] At the receiver, we used two directional antennas and ADL8142 Low Noise Amplifiers (LNA) to amplify the signal. We used Mini-Circuits ZMDB-44H-K+ RF mixers to mix the received signal with the transmitting signal. ZFHP-0R50-S+ and ZFHP-0R23-S+ are used to implement a band-pass filters (BPF). The output of the filters is fed to a Keysight DSOX3102G oscilloscope controlled by a laptop to capture and process the baseband signal. The waveform generator and oscilloscope are synchronized externally. Two points worth mentioning. First, we have used Mi-Wave 261(34)-20/595 horn antennas with 20dB gain and mechanically steered the AP's beams. However, one can instead use a phased array to electronically steer the AP's beams. Second, we have used a Keysight waveform generator and oscilloscope in our setup since they provide more flexibility for debugging and evaluating the end-to-end performance of the system. However, one can simply design a complete MilBack's AP using off-the-shelf components. In fact, all components required for our AP are common in most commercial mmWave radars such as the ones used in automobiles [47].

9 EVALUATION
We first evaluate the performance of different components of MilBack. We then evaluate the performance of complete MilBack in an indoor environment, with the presence of objects such as tables, chairs, and shelves.

---

[2]The maximum bandwidth of our signal generator is 2 GHz. We transmitted two 2 GHz chirps centered at 27.25 GHz and 28.75 GHz, respectively, and patch the results together.
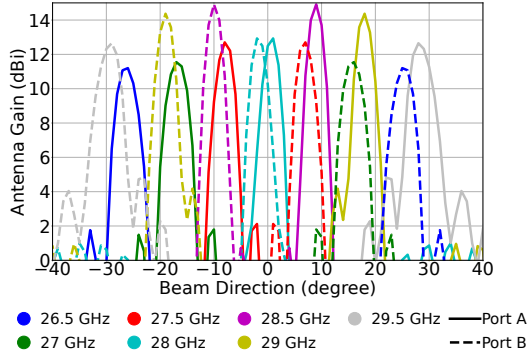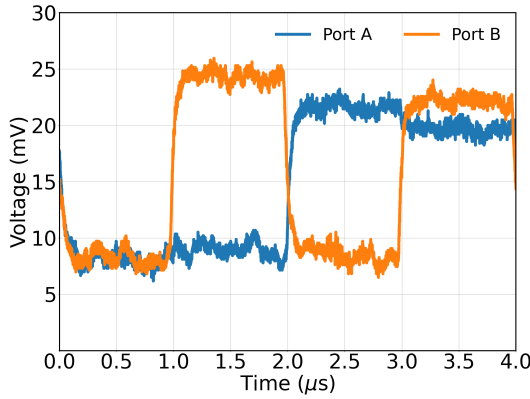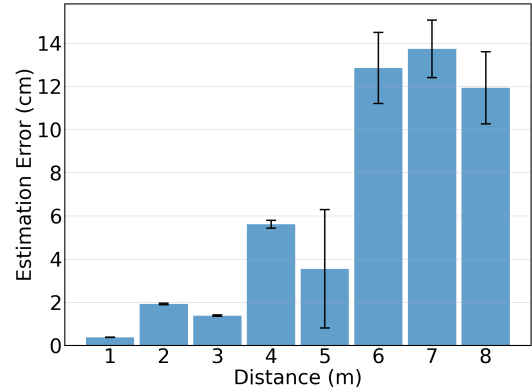
Figure 10: Dual-port FSA Beam Pattern.

Figure 11: OAQFM Micro-benchmark Signals at the node's FSA ports when symbols 00, 01, 10, 11 was sent by the AP.

(a) Ranging Accuracy

(b) Angle Accuracy

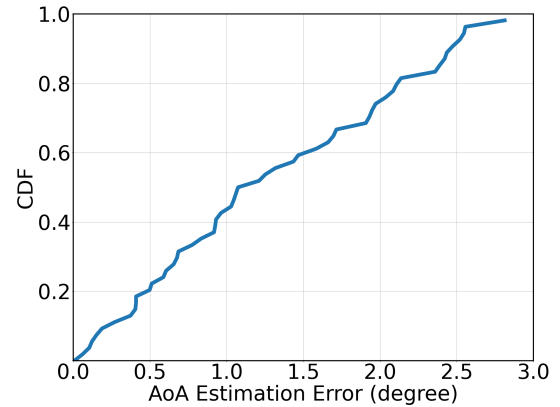**Figure 12: Localization Performance**

9.1 Microbenchmarks

Dual-port FSA We evaluate the beamforming performance of MilBack's dual-port FSA using HFSS. Figure 10 shows the beam pattern of each FSA port. Note, FSA steer beams continuously, however, we only plot the beams for seven sample frequencies. These results show that the FSA is able to create two sets of beams with more than 10dB gain where the direction of each beam depends on the frequency of the signal. Moreover, the direction of the beam for each port can change as much as 60 degrees when we change the frequency of the signal over our FMCW bandwidth (i.e. 26.5 GHz to 29.5 GHz).

OAQFM As mentioned in section 6.2, MilBack introduces the OAQFM modulation scheme for communication. Here, we provide the microbenchmark for this modulation scheme. We place a MilBack's node 2 m away from the AP. The AP estimates the orientation of the node and finds 27.5 GHz and 28.5 GHz as the correct signal frequencies to send data to the node. The AP then sends symbols "00", "01", "10" and "11", consecutively. In particular, the transmitter first sends nothing for a symbol duration (i.e. $1\mu s$ in this experiment). It then sends a single tone at 27.5 GHz for a symbol duration and another single tone at 28.5 GHz for another symbol duration. Finally, it sends two tones simultaneously. Figure

11 shows the output voltage of the envelope detectors at two ports of the FSA. This result shows that MilBack's node has successfully separated the two tones from each other at two different FSA ports. Moreover, the envelope detector at each FSA port has been able to measure the presence or absence of the mmWave signal, enabling the micro-controller to decode the bits.

9.2 Localization Performance

We evaluate the localization performance of MilBack. To localize a node in a 2-D plane, the AP needs to find the distance and angle of the node with respect to itself. In this experiment, we place our node at various angles and distances with respect to the AP while the AP transmits its signal and estimates the location of the node. In particular, to measure the distance, the AP uses the FMCW technique as described in section 5, and to measure the angle, the AP compares the phase of the node's baseband signal at two AP's antennas and uses that to estimate the direction of the node. We perform this experiment for different node to AP distances. For each distance, we repeat the experiment 20 times. We measure the ground truth using a BOSCH Laser meter and a protractor.

Figure 12a shows the mean and 90th percentile error in estimating the distance of the node with respect to the AP. As distance increases, the accuracy of the system decreases since the SNR of

the signal degrades. However, the mean accuracy is less than 5 cm and 12 cm, even when the node is 5 m and 8 m away, respectively. Figure 12b shows the CDF of the error in estimating the angle of the node with respect to the AP. The median and 90th percentile errors are 1.1 and 2.5 degrees, respectively. Note, the angel estimation can also be further improved if the AP uses a phased array with a large number of elements.
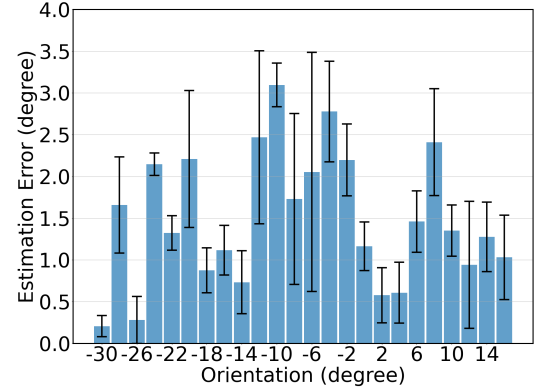
9.3 Orientation Performance

Next, we evaluate MilBack's Orientation Sensing performance. Recall that our orientation estimation is performed at both the AP and Node side; therefore, we evaluate them separately.

Orientation Sensing at Node In this experiment, the AP transmits the triangular FMCW pulses as described in section 8. We place the node at 2 m from the AP. Both ports of the node are set to absorptive mode, where the micro-controller samples the output of the envelop detectors at 1 MHz and measures the time separation between the two peaks on each port to estimate the orientation of the node using the technique described in section 5.2. The estimation from two ports is averaged to produce the final estimation of the node orientation. We perform this experiment for different orientations of the node. For each orientation, we repeat the experiment 25 times. We measure the ground truth using a protractor.

Figure 13a shows the mean and variance of error in estimating the orientation of the node for different orientations. The results show that the mean error in orientation estimation is always less than 3 degrees, which is sufficient for many IoT applications. For comparison, smartphones can estimate the orientation of the device with error between 0.5 and 3 degree [25].

Orientation Sensing at AP Next, we evaluate how accurately the AP can estimate the orientation of the node. To do so, we put the node 2 m away from the AP. The AP transmits an FMCW signal and estimate the node's orientation as described in 9.2. We perform this experiment for different orientation of the node. For each orientation, we repeat the experiment 25 times. We measure the ground truth using a protractor.

Figure 13b shows the mean and variance of the error in estimating the orientation of the node by the AP. In general, the mean error is less than 1.5 degree for all orientation. However, the error is slightly higher for orientations between $-6°$ and $-2°$. This is because that the mirror reflection of the FSA structure (created by its ground plane) is colliding on the modulated backscatter reflection. The mirror reflection increases the interference in our system. Ideally the mirror reflection should be removed by background subtraction technique, however, since it is varying due to the node switching, it will not be removed completely. Despite this issue, the AP can still estimate the orientation of the node with less than 3 degree error in average. As mentioned in Section 6, the AP use the orientation estimation to detect which signal frequency to use for OAQFM modulation scheme. However, as the beam width of the node is around 10 degree, 3-4 degree error in estimating the node's orientation will not impact on the performance of communication as we evaluate next.

(a) Orientation Estimation at the Node
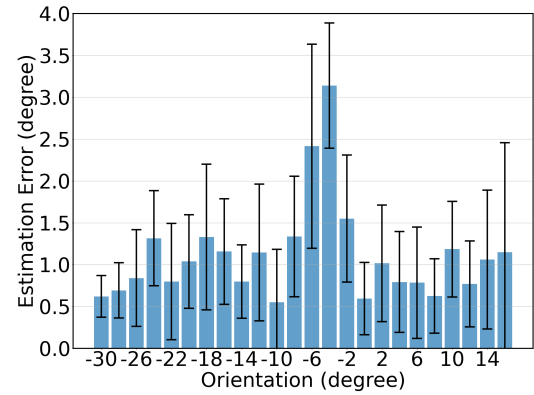
(b) Orientation Estimation at the AP

Figure 13: Orientation Estimation Performance

9.4 Downlink Performance

Next, we evaluate MilBack's performance in establishing a communication link from the AP to the node. Recall that we use OAQFM modulation scheme for downlink communication, where the AP sends data to the node using the presence or absence of two tones as described in section 6. The frequencies of these two tones depend on the orientation of the node which are estimated in the orientation sensing phase. In this experiment, we place the node at a fixed location. Then, the AP first finds the correct frequencies for two tones and sends its bits to the nodes using OAQFM scheme. The node receives the AP's signal using its FSA antenna and passes it to the envelop detectors which are connected to the micro-controller. We measure the Signal-to-Interference-plus-Noise Ratio (SINR) of the signal at the input of the micro-controller. Note, we measure SINR instead of SNR since the beam created by each port has side-lopes which may be on the same direction as the main beam of the other port. This non-ideality results in a small interference between the signals of two ports. Hence, we report our results in terms of SINR (instead of SNR) to count for both noise and this interference.

Figure 14 shows the result of this experiment across different distances of the node with respect to the AP for downlink bandwidth of 1 GHz. The figure shows that as the distance between the node and the AP increases, the SINR is reduced. However, MilBack
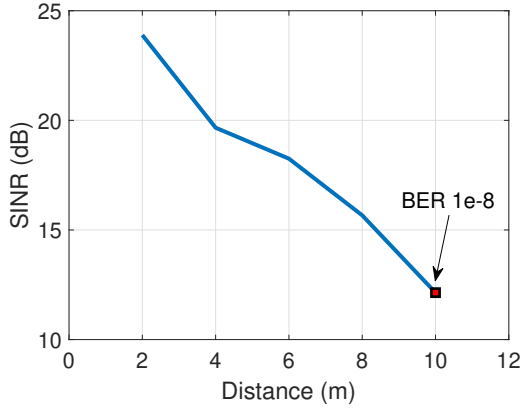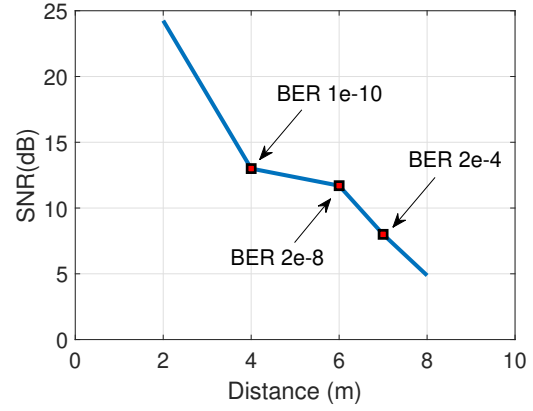
Figure 14: Downlink Performance

enables SINR of more than 12 dB even when the node is 10 m away from the AP. This SINR is more than enough to enable very low BER (i.e. less than 10^{-8}). Finally it is worth mentioning that the maximum downlink data rate of MilBack is 36 Mbps, which is mainly limited by the rise and fall time of the envelop detector. Hence, one can increase the data-rate further by using faster envelop detector. Another option is to define denser OAQFM modulation schemes, where each symbol represent more bits by considering different amplitudes for each tone of OAQFM.
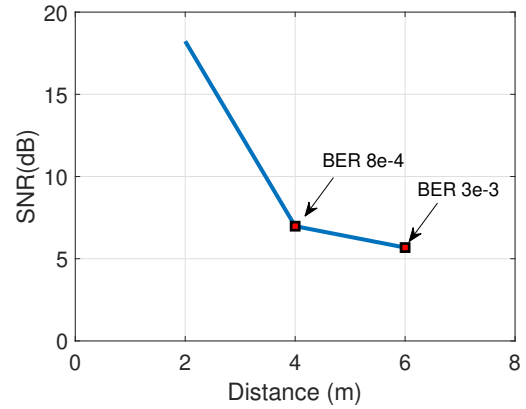
9.5 Uplink Performance

Finally, we evaluate the performance of MilBack in enabling uplink communication between the node and the AP. We place the node at a fixed location with respect to the AP. The AP first estimates the orientation of the node and uses it to find the correct frequencies for two tones. Then, the AP transmits a query signal consist of these tones as described. The node piggybacks its data on the query signal by switching each port of its FSA between reflective and absorptive mode. The AP receives the node's reflection, and separate it from the interference by downconverting it to the baseband signal for decoding as described in section 6.

Figure 15 shows the SNR of the node's signal at the AP across different distances for uplink data-rate of 10 Mbps and 40 Mbps. Note as the data-rate increases, the operating bandwidth increases. Higher bandwidth results in higher noise floor and lower SNR. The figure also shows the corresponding BER for each SNR. This results show that MilBack achieves a very low BER for uplink data-rate of 10 Mbps and 40 Mbps even when the node is 8 m and 6 m away from the AP, respectively. Note, the maximum uplink data rate that the node can operate is 160 Mbps. This rate is limited by switching speed of the node's switches. One can increase the uplink data-rate by using a faster switches and improve the range (or BER) by using larger FSAs with higher gains. Finally, it is worth mentioning that MilBack achieves higher SNR in downlink compared to the uplink. This is due the fact that in uplink the signal gets attenuated by the channel twice as opposed to downlink in which the signal goes through the channel once. However, for both uplink and downlink, MilBack's novel design enables very low-power communication.

(a) data-rate of 10 Mbps

(b) data-rate of 40 Mbps

Figure 15: Uplink Performance

9.6 Power Consumption

A key promise of MilBack is that it enables low-power two-way mmWave communication and localization for devices with limited energy resources. We evaluate the power consumption of MilBack 's node in different modes. The design of MilBack 's node is mostly using passive components and do not require any power hungry mmWave components such as amplifiers, mixers and oscillators. The only active components used in the design are two switches and two envelop detectors which are simple and low-power. The total power consumption of a MilBack's node is 18 mW during localization and downlink, and 32 mW during uplink.[3] The higher power consumption of uplink is due to the fact that switches are operating at higher rates. Note, considering the downlink and uplink data rate of 36 Mbps and 40 Mbps, the energy efficiency of MilBack is 0.5 nJ/bits and 0.8 nJ/bit, respectively. This is much lower than the energy efficiency of past mmWave backscatter networks which consume 2.4 nJ/bit while they only support uplink [35].

---

[3]Note, this power consumption does not include the power consumption of the micro-controller since it is already available in the user devices such as AR headsets and most IoTs. A typical micro-controller such as the one used in our prototype consumes 5.76 mW.

Systems	Uplink Communication	Localization	Downlink Communication	Orientation Sensing
mmTag [35]	Yes	No	No	No
Millimetro [45]	No	Yes	No	No
Omniscatter [12]	Yes	Yes	No	No
MilBack (This Work)	**Yes**	**Yes**	**Yes**	**Yes**

Table 1: Comparison with the state-of-the-art mmWave backscatter systems.

10 RELATED WORK

The related work can be divided to two groups: (a) mmWave and backscater communication, and (b) Integrated sensing and communication.

a) mmWave and Backscatter Communication: mmWave spectrum offers multi-GHz of licensed and unlicensed bandwidth that promises orders of magnitude higher networks throughput in the next generation communication network [14, 34, 40, 48, 51]. Therefore, a wide range of applications have been proposed for this technology such as Virtual Reality (VR) [6, 17], data center networks [16], and vehicular networks [18, 19, 49]. Moreover, due to the availability of large bandwidth and short wave length of mmWave signals, this technology can enable very accurate localization, enabling applications such as tracking and gesture sensing [27, 32, 53]. However, most existing mmWave work focus on applications which have substantial energy and computing power. Therefore today's mmWave systems are not suitable for applications with limited energy sources.

Over the past decade, there has been a significant amount of work on Backscatter technology. This technology is the most energy-efficient method for wireless communication. The most popular backscatter system is RFID which operates at 900 MHz band [38, 52]. Recently, researchers have proposed backscatter systems operating on WiFi band [7, 13, 22, 56]. However, none of these systems enable accurate localization, and high-data-rate uplink and downlink together. Moreover, these system operate in sub-6Ghz bands which are already congested.

Researchers have recently proposed mmWave backscatter system which brings mmWave technology to low-power devices which have limited energy and computations resources [12, 24, 35, 41, 45]. However, past work either enables accurate localization of the backscatter node or provide only uplink communication. In contrast, MilBack is the first mmWave backscatter system which provides accurate localization, uplink and downlink communication. Table 1 shows the features of MilBack comparing with the state-of-the-art mmWave backscatter systems.

b) Integrated Sensing and Communication (ISAC): Integrated Sensing and Communication (ISAC) is an emerging trend in the wireless community aiming at designing wireless systems that have both communication and sensing functionalities [29, 36]. The benefits of an integrated design are two-fold: 1) Integration Gain: sensing and communication modules share the wireless resources, such as transceiver and spectrum. 2) Coordination Gain: The sensing and communication modules share information to mutually benefit each other [15, 29].

Past work attempt to adapt existing sensing or communication systems and enable joint communication and sensing using different techniques such as designing novel waveforms [30, 31, 33] or algorithms to adopt OFMD waveform for sensing besides communication [46]. In contrast to past work which are mostly theoretical or focus on non-backscatter systems, MilBack is the first mmWave backscatter system that performs localization, orientation sensing, uplink and downlink communication.

11 CONCLUDING REMARKS

mmWave backscatter technology promises to bring mmWave connectivity to devices with limited energy resources such as IoT devices. However, existing mmWave backscatter systems enable either accurate localization or uplink communication. Hence, they are not suitable for most applications since they cannot enable downlink. This paper introduces MilBack, the first mmWave backscatter system which enables orientation sensing, localization, uplink and downlink. MilBack achieves this by proposing a novel architecture and modulation scheme for mmWave backscatter nodes. We believe with the advancement of mmWave backscatter systems, future mmWave access points (such as 5G/6G access points) and radars (such as automobile radars) can directly communicate to low-power IoT devices using mmWave signals. Finally, it is worth mentioning that MilBack is very low-power (i.e. consumes only 18 mW) while achieving 8 m range and 40 Mbps data-rate. This range and data-rate is sufficient for most IoT applications. However, both range and data-rate can be further increased by designing a larger FSA and faster switches in our prototype, respectively.

REFERENCES

[1] 2016. *FCC Opens Millimeter Wave Spectrum for 5G*. https://www.cooley.com/news/insight/2016/2016-07-14-fcc-opens-millimeter-wave-spectrum-for-5g Accessed: 2023-07-08.

[2] 2023. Datasheet Envelope Detector ADL6010. https://www.analog.com/media/en/technical-documentation/data-sheets/ADL6010.pdf. (2023). Accessed: 2023-07-08.

[3] 2023. Datasheet Microcontroller MSP-EXP430FR6989. https://www.ti.com/lit/ds/symlink/msp430fr6989.pdf. (2023). Accessed: 2023-07-08.

[4] 2023. Datasheet Power Amplifier ADPA7005. https://www.analog.com/media/en/technical-documentation/data-sheets/adpa7005chip.pdf. (2023). Accessed: 2023-07-08.

[5] 2023. Datasheet SPDT ADRF5020. https://www.analog.com/media/en/technical-documentation/data-sheets/ADRF5020.pdf. (2023). Accessed: 2023-07-08.

[6] Omid Abari, Dinesh Bharadia, Austin Duffield, and Dina Katabi. 2017. Enabling {High-Quality} Untethered Virtual Reality. In *14th USENIX Symposium on Networked Systems Design and Implementation (NSDI 17)*. 531–544.

[7] Ali Abedi, Farzan Dehbashi, Mohammad Hossein Mazaheri, Omid Abari, and Tim Brecht. 2020. WiTAG: Seamless WiFi Backscatter Communication. In *Proceedings*

of the Annual Conference of the ACM Special Interest Group on Data Communication on the Applications, Technologies, Architectures, and Protocols for Computer Communication (SIGCOMM '20). Association for Computing Machinery, New York, NY, USA, 240–252. https://doi.org/10.1145/3387514.3405866

[8] Fadel Adib, Chen-Yu Hsu, Hongzi Mao, Dina Katabi, and Frédo Durand. 2015. Capturing the human figure through a wall. *ACM Transactions on Graphics (TOG)* 34, 6 (2015), 1–13.

[9] Fadel Adib, Zachary Kabelac, and Dina Katabi. 2015. Multi-person localization via {RF} body reflections. In *12th {USENIX} Symposium on Networked Systems Design and Implementation ({NSDI} 15).* 279–292.

[10] Fadel Adib, Zach Kabelac, Dina Katabi, and Robert C Miller. 2014. 3D tracking via body radio reflections. In *11th USENIX Symposium on Networked Systems Design and Implementation (NSDI 14).* 317–329.

[11] Fadel Adib, Hongzi Mao, Zachary Kabelac, Dina Katabi, and Robert C Miller. 2015. Smart homes that monitor breathing and heart rate. In *Proceedings of the 33rd annual ACM conference on human factors in computing systems.* 837–846.

[12] Kang Min Bae, Namjo Ahn, Yoon Chae, Parth Pathak, Sung-Min Sohn, and Song Min Kim. 2022. OmniScatter: Extreme Sensitivity MmWave Backscattering Using Commodity FMCW Radar. In *Proceedings of the 20th Annual International Conference on Mobile Systems, Applications and Services (MobiSys '22).* Association for Computing Machinery, New York, NY, USA, 316–329. https://doi.org/10.1145/3498361.3538924

[13] Dinesh Bharadia, Kiran Raj Joshi, Manikanta Kotaru, and Sachin Katti. 2015. Backfi: High throughput wifi backscatter. *ACM SIGCOMM Computer Communication Review* 45, 4 (2015), 283–296.

[14] Sherif Adeshina Busari, Kazi Mohammed Saidul Huq, Shahid Mumtaz, Linglong Dai, and Jonathan Rodriguez. 2018. Millimeter-Wave Massive MIMO Communication for Future Wireless Systems: A Survey. *IEEE Communications Surveys & Tutorials* 20, 2 (2018), 836–869. https://doi.org/10.1109/COMST.2017.2787460

[15] Yuanhao Cui, Fan Liu, Xiaojun Jing, and Junsheng Mu. 2021. Integrating sensing and communications for ubiquitous IoT: Applications, trends, and challenges. *IEEE Network* 35, 5 (2021), 158–167.

[16] Yong Cui, Shihan Xiao, Xin Wang, Zhenjie Yang, Shenghui Yan, Chao Zhu, Xiang-Yang Li, and Ning Ge. 2017. Diamond: Nesting the data center network with wireless rings in 3-d space. *IEEE/ACM Transactions On Networking* 26, 1 (2017), 145–160.

[17] Mohammed S Elbamby, Cristina Perfecto, Mehdi Bennis, and Klaus Doppler. 2018. Toward low-latency and ultra-reliable virtual reality. *IEEE Network* 32, 2 (2018), 78–84.

[18] Kayhan Zrar Ghafoor, Linghe Kong, Sherali Zeadally, Ali Safaa Sadiq, Gregory Epiphaniou, Mohammad Hammoudeh, Ali Kashif Bashir, and Shahid Mumtaz. 2020. Millimeter-wave communication for internet of vehicles: Status, challenges, and perspectives. *IEEE Internet of Things Journal* 7, 9 (2020), 8525–8546.

[19] Marco Giordani, Andrea Zanella, and Michele Zorzi. 2017. Millimeter wave communication in vehicular networks: Challenges and opportunities. In *2017 6th International Conference on Modern Circuits and Systems Technologies (MOCAST).* IEEE, 1–6.

[20] Shuangfeng Han, I Chih-Lin, Zhikun Xu, and Corbett Rowell. 2015. Large-scale antenna systems with hybrid analog and digital beamforming for millimeter wave 5G. *IEEE Communications Magazine* 53, 1 (2015), 186–194.

[21] Shaya Karimkashi and Guifu Zhang. 2013. A dual-polarized series-fed microstrip antenna array with very high polarization purity for weather measurements. *IEEE transactions on antennas and propagation* 61, 10 (2013), 5315–5319.

[22] Bryce Kellogg, Aaron Parks, Shyamnath Gollakota, Joshua R Smith, and David Wetherall. 2014. Wi-Fi backscatter: Internet connectivity for RF-powered devices. In *Proceedings of the 2014 ACM conference on SIGCOMM.* 607–618.

[23] Kerim Kibaroglu, Mustafa Sayginer, Thomas Phelps, and Gabriel M Rebeiz. 2018. A 64-element 28-GHz phased-array transceiver with 52-dBm EIRP and 8–12-Gb/s 5G link at 300 meters without any calibration. *IEEE Transactions on Microwave Theory and Techniques* 66, 12 (2018), 5796–5811.

[24] John Kimionis, Apostolos Georgiadis, and Manos M Tentzeris. 2017. Millimeter-wave backscatter: A quantum leap for gigabit communication, RF sensing, and wearables. In *2017 IEEE MTT-S International Microwave Symposium (IMS).* IEEE, 812–815.

[25] Tim Kuhlmann, Pablo Garaizar, and Ulf-Dietrich Reips. 2021. Smartphone sensor accuracy varies from device to device in mobile research: The case of spatial orientation. *Behavior research methods* 53 (2021), 22–33.

[26] Thomas H Lee. 2003. *The design of CMOS radio-frequency integrated circuits.* Cambridge university press.

[27] Filip Lemic, James Martin, Christopher Yarp, Douglas Chan, Vlado Handziski, Robert Brodersen, Gerhard Fettweis, Adam Wolisz, and John Wawrzynek. 2016. Localization as a feature of mmWave communication. In *2016 International Wireless Communications and Mobile Computing Conference (IWCMC).* 1033–1038. https://doi.org/10.1109/IWCMC.2016.7577201

[28] Tianxiang Li, Mohammad Hossein Mazaheri, and Omid Abari. 2022. 5G in the Sky: The Future of High-Speed Internet via Unmanned Aerial Vehicles. In *Proceedings of the 23rd Annual International Workshop on Mobile Computing Systems and Applications (HotMobile '22).* Association for Computing Machinery, New York,

[29] Fan Liu, Yuanhao Cui, Christos Masouros, Jie Xu, Tony Xiao Han, Yonina C Eldar, and Stefano Buzzi. 2022. Integrated sensing and communications: Towards dual-functional wireless networks for 6G and beyond. *IEEE journal on selected areas in communications* (2022).

[30] Fan Liu, Christos Masouros, Ang Li, Huafei Sun, and Lajos Hanzo. 2018. MU-MIMO communications with MIMO radar: From co-existence to joint transmission. *IEEE Transactions on Wireless Communications* 17, 4 (2018), 2755–2770.

[31] Fan Liu, Longfei Zhou, Christos Masouros, Ang Li, Wu Luo, and Athina Petropulu. 2018. Toward dual-functional radar-communication systems: Optimal waveform design. *IEEE Transactions on Signal Processing* 66, 16 (2018), 4264–4279.

[32] Haipeng Liu, Yuheng Wang, Anfu Zhou, Hanyue He, Wei Wang, Kunpeng Wang, Peilin Pan, Yixuan Lu, Liang Liu, and Huadong Ma. 2020. Real-Time Arm Gesture Recognition in Smart Home Scenarios via Millimeter Wave Sensing. *Proc. ACM Interact. Mob. Wearable Ubiquitous Technol.* 4, 4, Article 140 (dec 2020), 28 pages. https://doi.org/10.1145/3432235

[33] Xiang Liu, Tianyao Huang, Nir Shlezinger, Yimin Liu, Jie Zhou, and Yonina C Eldar. 2020. Joint transmit beamforming for multiuser MIMO communications and MIMO radar. *IEEE Transactions on Signal Processing* 68 (2020), 3929–3944.

[34] Mohammad H. Mazaheri, Soroush Ameli, Ali Abedi, and Omid Abari. 2019. A Millimeter Wave Network for Billions of Things. In *Proceedings of the ACM Special Interest Group on Data Communication (SIGCOMM '19).* Association for Computing Machinery, New York, NY, USA, 174–186. https://doi.org/10.1145/3341302.3342068

[35] Mohammad Hossein Mazaheri, Alex Chen, and Omid Abari. 2021. MmTag: A Millimeter Wave Backscatter Network. In *Proceedings of the 2021 ACM SIGCOMM 2021 Conference (SIGCOMM '21).* Association for Computing Machinery, New York, NY, USA, 463–474. https://doi.org/10.1145/3452296.3472896

[36] Kumar Vijay Mishra, M.R. Bhavani Shankar, Visa Koivunen, Bjorn Ottersten, and Sergiy A. Vorobyov. 2019. Toward Millimeter-Wave Joint Radar Communications: A Signal Processing Perspective. *IEEE Signal Processing Magazine* 36, 5 (2019), 100–114. https://doi.org/10.1109/MSP.2019.2913173

[37] Kyriakos Neophytou, Matthias Steeg, Jonas Tebart, Andreas Stöhr, Stavros Iezekiel, and Marco A Antoniades. 2022. Simultaneous user localization and identification using leaky-wave antennas and backscattering communications. *IEEE Access* 10 (2022), 37097–37108.

[38] Jin-Ping Niu and Geoffrey Ye Li. 2019. An overview on backscatter communications. *Journal of Communications and Information Networks* 4, 2 (2019), 1–14.

[39] Yong Niu, Yong Li, Depeng Jin, Li Su, and Athanasios V Vasilakos. 2015. A survey of millimeter wave communications (mmWave) for 5G: opportunities and challenges. *Wireless networks* 21, 8 (2015), 2657–2676.

[40] Yong Niu, Yong Li, Depeng Jin, Li Su, and Athanasios V. Vasilakos. 2015. A Survey of Millimeter Wave Communications (MmWave) for 5G: Opportunities and Challenges. *Wirel. Netw.* 21, 8 (nov 2015), 2657–2676. https://doi.org/10.1007/s11276-015-0942-z

[41] John Nolan, Kun Qian, and Xinyu Zhang. 2021. RoS: Passive Smart Surface for Roadside-to-Vehicle Communication. In *Proceedings of the 2021 ACM SIGCOMM 2021 Conference (SIGCOMM '21).* Association for Computing Machinery, New York, NY, USA, 165–178. https://doi.org/10.1145/3452296.3472896

[42] Sandeep Rao. 2017. Introduction to mmWave sensing: FMCW radars. *Texas Instruments (TI) mmWave Training Series* (2017), 1–11.

[43] David J Richardson, John M Fini, and Lynn E Nelson. 2013. Space-division multiplexing in optical fibres. *Nature photonics* 7, 5 (2013), 354–362.

[44] E Sharp and M Diab. 1960. Van Atta reflector array. *IRE Transactions on Antennas and Propagation* 8, 4 (1960), 436–438.

[45] Elahe Soltanaghaei, Akarsh Prabhakara, Artur Balanuta, Matthew Anderson, Jan M. Rabaey, Swarun Kumar, and Anthony Rowe. 2021. Millimetro: mmWave Retro-Reflective Tags for Accurate, Long Range Localization. In *Proceedings of the 27th Annual International Conference on Mobile Computing and Networking (MobiCom '21).* Association for Computing Machinery, New York, NY, USA, 69–82. https://doi.org/10.1145/3447993.3448627

[46] Christian Sturm and Werner Wiesbeck. 2011. Waveform design and signal processing aspects for fusion of wireless communications and radar sensing. *Proc. IEEE* 99, 7 (2011), 1236–1259.

[47] Texas Instrument 2022. *AWRL6432 Single-Chip 57- to 64-GHz Automotive Radar Sensor.* Texas Instrument. https://www.ti.com/lit/ds/symlink/awrl6432.pdf?ts=1676366347705&ref_url=https%253A%252F%252Fwww.ti.com%252Fsensors%252Fmmwave-radar%252Fautomotive%252Fproducts.html

[48] Anthony Ngozichukwuka Uwaechia and Nor Muzlifah Mahyuddin. 2020. A Comprehensive Survey on Millimeter Wave Communications for Fifth-Generation Wireless Networks: Feasibility and Challenges. *IEEE Access* 8 (2020), 62367–62414. https://doi.org/10.1109/ACCESS.2020.2984204

[49] Vutha Va, Takayuki Shimizu, Gaurav Bansal, Robert W Heath Jr, et al. 2016. Millimeter wave vehicular communications: A survey. *Foundations and Trends® in Networking* 10, 1 (2016), 1–113.

[50] Mojtaba Vaezi, Zhiguo Ding, and H Vincent Poor. 2019. *Multiple access techniques for 5G wireless networks and beyond.* Vol. 159. Springer.

[51] Xiong Wang, Linghe Kong, Fanxin Kong, Fudong Qiu, Mingyu Xia, Shlomi Arnon, and Guihai Chen. 2018. Millimeter Wave Communication: A Comprehensive Survey. *IEEE Communications Surveys & Tutorials* 20, 3 (2018), 1616–1653. https://doi.org/10.1109/COMST.2018.2844322

[52] Chenren Xu, Lei Yang, and Pengyu Zhang. 2018. Practical backscatter communication systems for battery-free Internet of Things: A tutorial and survey of recent research. *IEEE Signal Processing Magazine* 35, 5 (2018), 16–27.

[53] Hongfei Xue, Yan Ju, Chenglin Miao, Yijiang Wang, Shiyang Wang, Aidong Zhang, and Lu Su. 2021. MmMesh: Towards 3D Real-Time Dynamic Human Mesh Construction Using Millimeter-Wave. In *Proceedings of the 19th Annual International Conference on Mobile Systems, Applications, and Services (MobiSys '21)*. Association for Computing Machinery, New York, NY, USA, 269–282. https:

//doi.org/10.1145/3458864.3467679

[54] Han Yan, Sridhar Ramesh, Timothy Gallagher, Curtis Ling, and Danijela Cabric. 2019. Performance, power, and area design trade-offs in millimeter-wave transmitter beamforming architectures. *IEEE Circuits and Systems Magazine* 19, 2 (2019), 33–58.

[55] Sun Zhan-shan, Ren Ke, Chen Qiang, Bai Jia-jun, and Fu Yun-qi. 2017. 3D radar imaging based on frequency-scanned antenna. *IEICE Electronics Express* 14, 12 (2017), 20170503–20170503.

[56] Pengyu Zhang, Dinesh Bharadia, Kiran Joshi, and Sachin Katti. 2016. Hitchhike: Practical backscatter using commodity wifi. In *Proceedings of the 14th ACM Conference on Embedded Network Sensor Systems CD-ROM.* 259–271.